Author(s): Elomaa, Hanna; Härkönen, Jouni; Väyrynen, Sara A.; Ahtiainen, Maarit; Ogino, Shuji; Nowak, Jonathan A.; Lau, Mai Chan; Helminen, Olli; Wirta, Erkki-Ville; Seppälä, Toni T.; Böhm, Jan; Mecklin, Jukka-Pekka; Kuopio, Teijo; Väyrynen, Juha P.

Title: Quantitative multiplexed analysis of indoleamine 2,3-dioxygenase (IDO) and arginase-1 (ARG1) expression and myeloid cell infiltration in colorectal cancer

Year: 2024

Version: Published version

Please cite the original version:

Elomaa, H., Härkönen, J., Väyrynen, S. A., Ahtiainen, M., Ogino, S., Nowak, J. A., Lau, M. C., Helminen, O., Wirta, E.-V., Seppälä, T. T., Böhm, J., Mecklin, J.-P., Kuopio, T., & Väyrynen, J. P. (2024). Quantitative multiplexed analysis of indoleamine 2,3-dioxygenase (IDO) and arginase-1 (ARG1) expression and myeloid cell infiltration in colorectal cancer. Modern Pathology, 37(4), Article 100450. https://doi.org/10.1016/j.modpat.2024.100450

Mod Pathol 37 (2024) 100450

MODERN PATHOLOGY

USCAP UNITED STATES AND CANADIAN ACADEMY OF PATHOLOGY
Creating a Better Pathologist

Journal homepage: https://modernpathology.org/

Research Article

Quantitative Multiplexed Analysis of Indoleamine 2,3-Dioxygenase (IDO) and Arginase-1 (ARG1) Expression and Myeloid Cell Infiltration in Colorectal Cancer

Hanna Elomaa[a,b], Jouni Härkönen[c,d], Sara A. Väyrynen[e], Maarit Ahtiainen[c], Shuji Ogino[f,g,h,i], Jonathan A. Nowak[f], Mai Chan Lau[j,k], Olli Helminen[l], Erkki-Ville Wirta[m,n], Toni T. Seppälä[n,o,p,q], Jan Böhm[c], Jukka-Pekka Mecklin[b,r], Teijo Kuopio[a,c], Juha P. Väyrynen[l,*]

[a] *Department of Biological and Environmental Science, University of Jyväskylä, Jyväskylä, Finland;* [b] *Department of Education and Research, Hospital Nova of Central Finland, Well Being Services County of Central Finland, Jyväskylä, Finland;* [c] *Department of Pathology, Hospital Nova of Central Finland, Well Being Services County of Central Finland, Jyväskylä, Finland;* [d] *Faculty of Health Sciences, A.I. Virtanen Institute for Molecular Sciences, University of Eastern Finland, Kuopio, Finland;* [e] *Department of Internal Medicine, Oulu University Hospital, Oulu, Finland;* [f] *Program in Molecular Pathological Epidemiology, Department of Pathology, Brigham and Women's Hospital and Harvard Medical School, Boston, Massachusetts;* [g] *Department of Epidemiology, Harvard T.H. Chan School of Public Health, Boston, Massachusetts;* [h] *Broad Institute of MIT and Harvard, Cambridge, Massachusetts;* [i] *Cancer Immunology and Cancer Epidemiology Programs, Dana-Farber Harvard Cancer Center, Boston, Massachusetts;* [j] *Bioinformatics Institute (BII), Agency of Science, Technology and Research (A*STAR), Singapore, Singapore;* [k] *Singapore Immunology Network (SIgN), Agency of Science, Technology and Research (A*STAR), Singapore, Singapore;* [l] *Translational Medicine Research Unit, Medical Research Center Oulu, Oulu University Hospital, University of Oulu, Oulu, Finland;* [m] *Department of Gastroenterology and Alimentary Tract Surgery, Tampere University Hospital, Tampere, Finland;* [n] *Faculty of Medicine and Health Technology, Tampere University and Tays Cancer Center, Tampere University Hospital, Tampere, Finland;* [o] *Department of Gastrointestinal Surgery, Helsinki University Central Hospital, University of Helsinki, Helsinki, Finland;* [p] *Applied Tumor Genomics, Research Program Unit, University of Helsinki, Helsinki, Finland;* [q] *Abdominal Center, Helsinki University Hospital, Helsinki, Finland;* [r] *Faculty of Sport and Health Sciences, University of Jyväskylä, Jyväskylä, Finland*

ARTICLE INFO

Article history:
Received 19 October 2023
Revised 12 January 2024
Accepted 4 February 2024
Available online 16 February 2024

Keywords:
bioimage analysis
colorectal carcinoma
multiplex immunohistochemistry
prognostic factors
spatial analysis
tumor immunology

ABSTRACT

Indoleamine 2,3-dioxygenase (IDO) and arginase-1 (ARG1) are amino acid–metabolizing enzymes, frequently highly expressed in cancer. Their expression may deplete essential amino acids, lead to immunosuppression, and promote cancer growth. Still, their expression patterns, prognostic significance, and spatial localization in the colorectal cancer microenvironment are incompletely understood. Using a custom 10-plex immunohistochemistry assay and supervised machine learning–based digital image analysis, we characterized IDO and ARG1 expression in monocytic cells, granulocytes, mast cells, and tumor cells in 833 colorectal cancer patients. We evaluated the prognostic value and spatial arrangement of IDO- and ARG1-expressing myeloid and tumor cells. IDO was mainly expressed not only by monocytic cells but also by some tumor cells, whereas ARG1 was predominantly expressed by granulocytes. Higher density of IDO^+ monocytic cells was an independent prognostic factor for improved cancer-specific survival both in the tumor center ($P_{trend} = .0002$; hazard ratio [HR] for the highest ordinal category Q4 [vs Q1], 0.51; 95% CI, 0.33-0.79) and the invasive margin ($P_{trend} = .0015$). Higher density of granulocytes was associated with prolonged cancer-specific survival in univariable models, and higher $FCGR3^+ARG1^+$ neutrophil density in the tumor center also in multivariable analysis ($P_{trend} = .0020$). Granulocytes were, on average, located closer to tumor cells than monocytic cells. Furthermore, IDO^+ monocytic cells and $ARG1^-$ granulocytes were closer than IDO^- monocytic cells and $ARG1^+$ granulocytes, respectively. The mRNA expression of the *IDO1* gene was assessed in myeloid and tumor cells using publicly available single-cell RNA sequencing data for 62 colorectal cancers. *IDO1* was

* Corresponding author.
E-mail address: juha.vayrynen@oulu.fi (J.P. Väyrynen).

https://doi.org/10.1016/j.modpat.2024.100450

mainly expressed in monocytes and dendritic cells, and high *IDO1* activity in monocytes was associated with enriched immunostimulatory pathways. Our findings provided in-depth information about the infiltration patterns and prognostic value of cells expressing IDO and/or ARG1 in the colorectal cancer microenvironment, highlighting the significance of host immune response in tumor progression.

Introduction

Amino acid metabolism is often altered in cancer, and colorectal cancer is frequently associated with upregulated expression of amino acid–metabolizing enzymes indoleamine 2,3-dioxygenase (IDO) and arginase-1 (ARG1).[1,2] Tryptophan is an essential amino acid, which promotes T cell activation and proliferation. IDO plays an important role in the catabolism of tryptophan into kynurenine, leading to diminished tryptophan levels and potentially contributing to T cell suppression.[3] L-arginine is a semiessential amino acid, promoting the production of memory T cells and T cell survival. ARG1 is involved in the catabolism of L-arginine to L-ornithine and urea.[4] Increased expression of ARG1 may deplete L-arginine levels and thus lead to immunosuppression and cancer progression.[5] Some studies have found high expression of IDO and ARG1 to be associated with lower T cell activity, immune tolerance, metastasis, and poor clinical outcome in various tumors,[6,7] including colorectal cancer.[2,8,9] Thus, IDO and ARG1 are potential targets for cancer immunotherapy.

IDO is expressed by several cells in the tumor microenvironment, including monocytic cells, tumor cells, and endothelial cells,[3] whereas ARG1 is highly expressed by granulocytes.[10] The patterns of myeloid immune cell infiltration and IDO and ARG1 expression are heterogeneous between tumors, and their prognostic roles in colorectal cancer are still incompletely understood. Phenotyping myeloid cell subtypes using standard immunohistochemistry is challenging because of lack of single specific surface antigens,[11] but recent advances in multiplex immunohistochemistry have enabled detailed, spatially resolved analysis of multiple antigens at single-cell resolution.

In this study, we quantified the expression of IDO and ARG1 in monocytic cells, granulocytes, mast cells, and tumor cells in 833 colorectal cancers using a custom multiplexed immunohistochemistry assay and machine learning–based image analysis. We aimed to (1) characterize the expression patterns and prognostic value of IDO and ARG1 in the colorectal cancer microenvironment, (2) analyze the infiltration patterns and prognostic significance of myeloid cell subtypes, and (3) investigate the spatial proximity between IDO- and ARG1-expressing myeloid cells and tumor cells. We hypothesized that higher densities of IDO^+ and $ARG1^+$ myeloid cells and higher expression of IDO in tumor cells would be associated with shorter colorectal cancer-specific survival.

Material and Methods

Study Population

This study was based on an earlier described[12,13] cohort composing 1343 retrospectively collected primary tumor samples of colorectal cancer patients who underwent surgery during 2000-2015 in Central Finland Central Hospital, Jyväskylä, Finland. The study benefited from samples/data from Central Finland Biobank, Jyväskylä, Finland. In accordance with our previous studies,[12,13] we excluded patients who died within 30 days after surgery ($N = 40$) or had received preoperative radiotherapy, chemotherapy, or chemoradiotherapy ($N = 243$). After further excluding tumors with inadequate tumor tissue or unsuccessful multiplex immunohistochemistry staining either in the tumor center or in the invasive margin ($N = 346$), the final cohort included samples of 833 colorectal cancer patients (Table 1). These patients included two patients with known Lynch syndrome. All tumors were previously screened for mismatch repair (MMR) deficiency and *BRAF* V600E mutation with immunohistochemistry.[13] Furthermore, the densities of $CD3^+$ and $CD8^+$ T cells were previously analyzed using immunohistochemistry and machine learning–based image analysis.[13]

Multiplex Immunohistochemistry

Multiplex immunohistochemistry was conducted using tissue microarrays designed to contain 4 (2 tumor centers and 2 invasive margins) 1-mm diameter cores from each tumor.[13] We built a 10-plex immunohistochemistry assay to characterize IDO and ARG1 expression and myeloid cell infiltration in the colorectal cancer microenvironment. The panel included a myeloid cell marker (ITGAM [CD11b]) and markers for monocytic cells (CD14), granulocytes (CEACAM8 [CD66b]), mast cells (TPSAB1 [mast cell tryptase]), and tumor cells (KRT [keratin]). Additionally, IDO, ARG1, FCGR3 (CD16), HLADR, and CD33 were included. We follow the standardized nomenclature system for protein names recommended by the expert panel.[14]

The potential primary antibodies were screened based on their clinical use in the pathology laboratory of Hospital Nova (Jyväskylä, Finland) or their previous utilization in published literature. The characteristics and optimal dilutions of the antibodies were first tested using standard immunohistochemistry in a tissue microarray containing several cores from tonsils, normal colon mucosa, and colorectal adenocarcinomas. The cyclic 10-plex immunohistochemistry assay was then optimized, and the validity of the assay was confirmed by comparing the staining patterns of multiplex immunohistochemistry with those of standard single-plex immunohistochemistry (Supplementary Fig. S1).

The multiplex immunohistochemistry staining protocol, reagents, and the primary antibodies along with their dilutions and epitope retrieval conditions are shown in Supplementary Figure S2. All markers were sequentially stained with Bond-III automated immunohistochemistry stainer using a Bond Refine Detection kit (DS9800, Leica Biosystems), with 3,3'-diaminobenzidine replaced with 3-amino-9-ethylcarbazole. The tissue microarray specimens were cut at 3.5-μm thickness and stained in one batch to ensure uniform staining across all tissue microarrays (Supplementary Fig. S3). After each staining cycle, the slides were mounted with water-soluble mounting medium and

Table 1
Demographic and clinical characteristics of colorectal cancer cases according to the overall density of IDO$^+$ monocytic cells

Characteristic	Total *N*	IDO$^+$ monocytic cell density				
		Q1	Q2	Q3	Q4	*P*
All cases	833 (100%)	209 (25%)	208 (25%)	208 (25%)	208 (25%)	
Sex						.35
Female	411 (49%)	94 (45%)	103 (50%)	102 (49%)	112 (54%)	
Male	422 (51%)	115 (55%)	105 (50%)	106 (51%)	96 (46%)	
Age (y)						.12
<65	225 (27%)	68 (33%)	57 (27%)	53 (26%)	47 (23%)	
65-75	297 (36%)	71 (34%)	81 (39%)	77 (37%)	68 (33%)	
>75	311 (37%)	70 (34%)	70 (34%)	78 (38%)	93 (45%)	
Year of operation						< .0001
2000-2005	262 (31%)	62 (30%)	64 (31%)	65 (31%)	71 (34%)	
2006-2010	261 (31%)	89 (43%)	74 (36%)	53 (26%)	45 (22%)	
2011-2015	310 (37%)	58 (28%)	70 (34%)	90 (43%)	92 (44%)	
Tumor location						.072
Proximal colon	409 (49%)	91 (44%)	112 (54%)	92 (44%)	114 (55%)	
Distal colon	299 (36%)	86 (41%)	69 (33%)	84 (40%)	60 (29%)	
Rectum	125 (15%)	32 (15%)	27 (13%)	32 (15%)	34 (16%)	
AJCC stages						< .0001
I	143 (17%)	16 (8%)	41 (20%)	41 (20%)	45 (22%)	
II	317 (38%)	66 (32%)	65 (31%)	93 (45%)	93 (45%)	
III	270 (32%)	90 (43%)	64 (31%)	56 (27%)	60 (29%)	
IV	103 (12%)	37 (18%)	38 (18%)	18 (9%)	10 (5%)	
Tumor grade						.019
Low-grade (well to moderately differentiated)	704 (85%)	182 (87%)	177 (85%)	183 (88%)	162 (78%)	
High-grade (poorly differentiated)	129 (15%)	27 (13%)	31 (15%)	25 (12%)	46 (22%)	
Lymphovascular invasion						.0003
No	654 (79%)	144 (69%)	161 (77%)	174 (84%)	175 (84%)	
Yes	179 (21%)	65 (31%)	47 (23%)	34 (16%)	33 (16%)	
MMR status						< .0001
MMR proficient	705 (85%)	196 (94%)	184 (89%)	167 (80%)	158 (76%)	
MMR deficient	128 (15%)	13 (6%)	24 (12%)	41 (20%)	50 (24%)	
BRAF status						.12
Wild type	697 (84%)	181 (87%)	180 (87%)	171 (82%)	165 (79%)	
Mutant	136 (16%)	28 (13%)	28 (14%)	37 (18%)	43 (21%)	

AJCC, American Joint Committee on Cancer; MMR, mismatch repair.

scanned using an automated slide scanner equipped with a 20× objective. Destaining with ethanol and heat-mediated antibody stripping was performed before the sequential staining cycle, using the previously described method.[13]

Machine Learning-Based Cell and Tissue Phenotyping

Tissue microarray cores were recognized and separated into single-core images using the *TMA dearrayer* function in QuPath (0.2.3) image analysis software.[15] We removed all unrepresentative core images, which were fully or partly (less than 50% of the entire core area after all staining cycles present) detached or included a minimal amount of tumor tissue. Only representative cores with successful staining in all 10 staining cycles were included for further analyses. The single-core images were merged into 12-channel pseudoimmunofluorescence multiplex images (hematoxylin channels as the 1st and 12th, 10 multiplex immunohistochemistry staining channels as the 2nd to 11th) using the MultiStackReg macro (downloaded from: http://bradbusse.net/downloads.html) in Fiji/ImageJ software.[16] The hematoxylin channels were used for aligning nuclei of all core images. We followed previously used[13] principles for tissue microarray core selection criteria and for aligning single-core images into pseudoimmunofluorescence multiplex images. An example of the conversion of multiplex immunohistochemistry images into a 12-channel pseudoimmunofluorescence image is illustrated in Figure 1A, B.

Tissue compartments and cells were detected and phenotyped using previously validated[17] supervised machine learning–based algorithms in QuPath. The image analysis was performed blinded to the clinical data and following the main steps of a previous study.[12] We classified tissue compartments into tumor epithelium, stroma, and other (ignored from the analysis) using the built-in *pixel classifier* function. Cells were detected using the *cell detection* function and phenotyped into 5 main categories using the *object classifier* function: monocytic cells (CD14$^+$CEACAM8$^-$TBSAB1$^-$KRT$^-$), granulocytes (CD14$^-$CEACAM8$^+$TBSAB1$^-$KRT$^-$), mast cells (CD14$^-$CEACAM8$^-$TBSAB1$^+$KRT$^-$), tumor cells (CD14$^-$CEACAM8$^-$TBSAB1$^-$KRT$^+$), and other cells (CD14$^-$CEACAM8$^-$TBSAB1$^-$KRT$^-$) (Fig. 1C).

Further cell data processing, quantification, and statistical analyses were conducted in RStudio (1.3.1093) and R statistical programming (4.0.3, R Core Team) with packages *circlize* (0.4.15), *corrplot* (0.92), *ComplexHeatmap* (2.16.0), *ggplot2* (3.4.2), *ggpubr* (0.6.0), *gmodels* (2.18.1.1), *spatstat* (3.0-5), *survival* (3.5-5), *survminer* (0.4.9), and *tidyverse* (2.0.0). We categorized cells according to their cytoplasmic staining intensities of FCGR3 (Fc gamma receptor 3A, CD16), HLADR, IDO, and ARG1 by setting fixed cutoff values. We calculated cell densities (cells/mm^2) within the region of interest. The mean density was calculated when multiple cores were successfully analyzed from the same tumor region. IDO

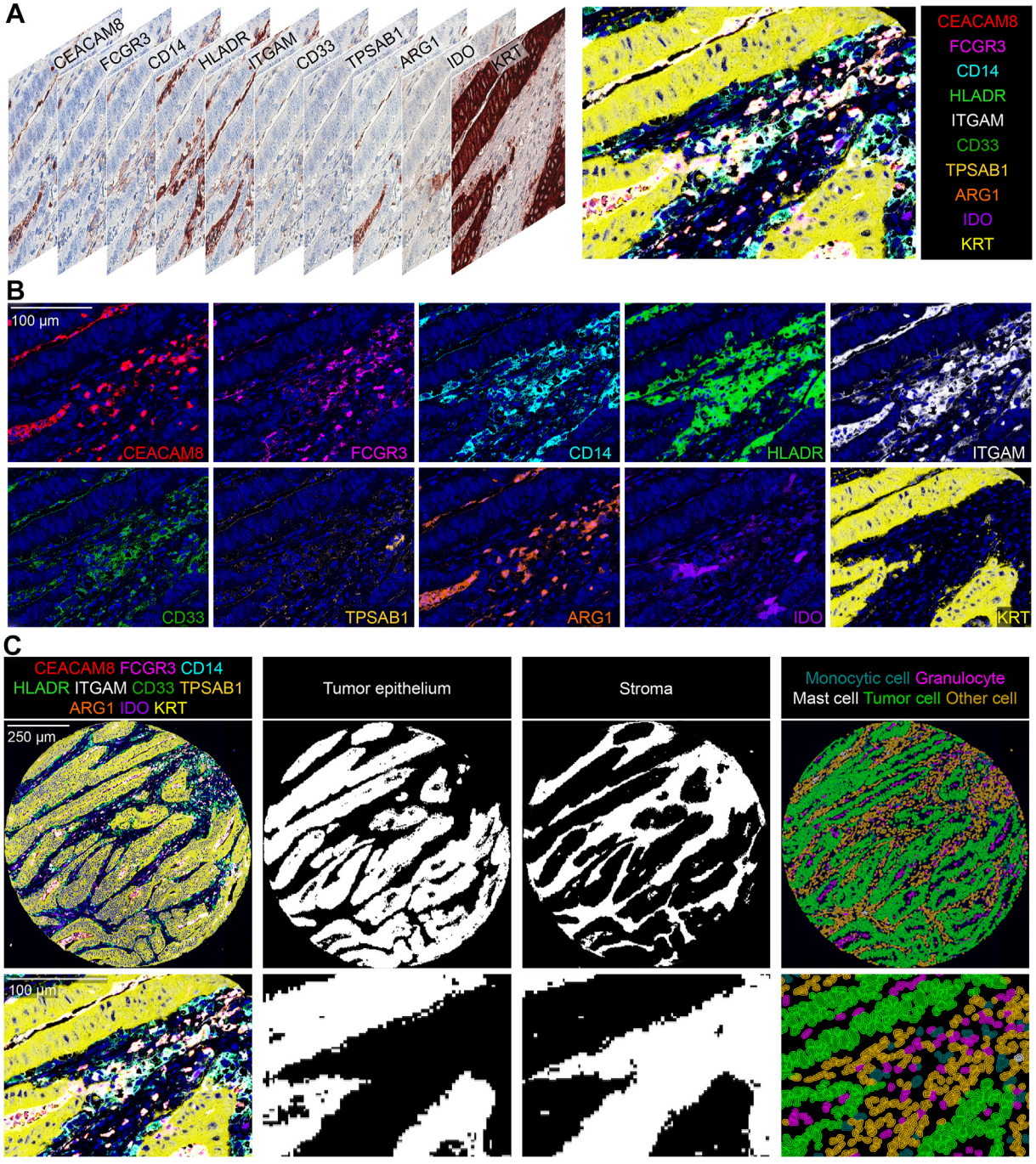

Figure 1.
Multiplex immunohistochemistry assay and machine learning–based image analysis. (A) Digitized multiplex immunohistochemistry images from each staining cycle were co-registered and converted into 10-plex pseudo-immunofluorescence images. (B) Each channel of a 10-plex pseudo-immunohistochemistry image represented separately. (C) Machine learning–based image analysis for detecting and classifying tissue compartments and cells in QuPath. Tissue compartments were classified into tumor epithelium and stroma. Cells were classified into monocytic cells, granulocytes, mast cells, tumor cells, and other cells.

expression in tumor cells was assessed by calculating the percentage of IDO^+ tumor cells relative to all tumor cells. Myeloid cell densities and IDO^+ tumor cell percentage were categorized into ordinal quartiles (Q1-Q4). In cell density variables with over 25% of zero cell densities, all zero densities were categorized as Q1, and the remaining values were divided equally into Q2 to Q4. All tumors with less than 1% of IDO^+ tumor cells were categorized as negative. To analyze spatial proximity between immune cells and tumor cells, we calculated nearest neighbor distances (NNDs). NND measures the distance from a specific point (eg, immune cell) to its closest neighbor point of a specific category (eg, tumor cell).

Statistical Analysis

The associations between categorical cell density variables and patient characteristics were tested using crosstabulation and the χ^2 test. The associations between continuous cell density variables

and patient characteristics were assessed with the Wilcoxon rank-sum test (comparing 2 classes) or the Kruskal-Wallis test (comparing more than 2 classes). Correlations between cell densities were assessed using Spearman's rank correlation test.

The survival outcomes were analyzed with univariable and multivariable Cox proportional hazard models for cancer-specific and overall survival, with cancer-specific survival as the primary survival endpoint. We limited the follow-up to 10 years, as Schoenfeld residual plots supported the proportionality of hazards during most of the follow-up period up to 10 years. The selection of variables for multivariable models was based on previous studies in this patient cohort[12,13] and included (reference category listed first) sex (male or female), age (<65, 65-75, and >75 years), year of operation (2000-2005, 2006-2010, and 2011-2015), tumor location (proximal colon, distal colon, and rectum), American Joint Committee on Cancer stages (I-II, III, and IV), tumor grade (well/moderately differentiated or poorly differentiated), lymphovascular invasion (negative or positive), MMR status (proficient or deficient), and *BRAF* status (wild type or mutant). Kaplan-Meier curves were used to visualize survival, and log-rank test was used to evaluate the statistical significance. In accordance with our previous studies,[12,13] P values < .005 were considered statistically significant based on the recommendation of an expert panel.[18]

Single-Cell RNA Transcriptomic Analysis for IDO1 Expression

We also assessed *IDO1* expression using publicly available single-cell data for 62 tumors. Single-cell RNA-seq counts and metadata were downloaded from Gene Expression Omnibus (GEO, GSID: GSE178341) and Broad Institute Single Cell Portal (https://singlecell.broadinstitute.org/single_cell, dataset c295). Single-cell data processing was conducted with *scCustomize* (1.1.3), *hdf5r* (1.3.8), and *Seurat* (1.3.8) R-packages. Only tumor samples were included in the analysis. Outlier cells were filtered by excluding those with more than 200 and less than 2500 features, as well as those with over 10% mitochondrial reads. Data were log-normalized and scaled with standard *Seurat* functions. Cell populations from the original publication[19] were used. For visual representation of the data, principal component analysis and uniform manifold approximation and projection were run with top 2500 variable features and 15 dimensions, respectively. *IDO1*-positive cells were classified as cells expressing over 1.5 log-normalized mRNA. Pathway analysis between *IDO1*$^+$ and *IDO1*$^-$ monocytes was computed with *fGSEA* (1.22) package for the differentially expressed genes assessed with *Seurat* function *FindMarkers* with *GO Biological Process* gene sets. To assess for differences in cellular interactions between different monocyte compositions, we computed *CellChat* (1.6.1) secretory interactions for the patients harboring either low or high fractions of IDO1+ monocytes (lower and higher quantiles, respectively).[20] Single-cell data visualization was conducted with *Seurat* and *CellChat* packages.

Results

Myeloid Cell Phenotypes and Density Analyses

We successfully analyzed 2813 tissue microarray cores for tumors of 833 colorectal cancer patients (mean, 3.4 per patient; SD, 0.71; tumor center, 1.8; SD, 0.43; and invasive margin, 1.6; SD, 0.52). Core-to-core correlations for myeloid cell densities were moderate to high both in the tumor center (R = 0.42-0.58) and in the invasive margin (R = 0.48-0.68) (Supplementary Fig. S4). We identified 24,310,185 cells across all tissue microarrays, of which 6.4% were monocytic cells, 3.9% were granulocytes, 1.4% were mast cells, and 42% were tumor cells.

We further classified monocytic cells according to HLADR and FCGR3 expression into mature CD14$^+$HLADR$^+$ and immature CD14$^+$HLADR$^-$ monocytic cells and into CD14$^+$FCGR3$^+$ and CD14$^+$FCGR3$^-$ monocytic cells. Granulocytes were further classified according to FCGR3 expression into FCGR3$^+$ neutrophils (CEACAM8$^+$FCGR3$^+$) and FCGR3$^-$ other granulocytes (CEACAM8$^+$FCGR3$^-$). The majority of CD14$^+$ monocytic cells were mature (HLADR$^+$, 84%) and more likely FCGR3$^+$ (65%) than FCGR3$^-$ (35%). Of CEACAM8$^+$ granulocytes, the majority (84%) were identified as FCGR3$^+$ neutrophils.

We evaluated the associations between myeloid cell densities and clinicopathologic features. Higher densities of monocytic cells and granulocytes were associated with proximal tumor location, high tumor grade, MMR deficiency, and *BRAF* mutation, whereas higher mast cell density was associated with low tumor grade, MMR proficiency, and absence of *BRAF* mutation. Both higher densities of granulocytes and mast cells were associated with low stage and absence of lymphovascular invasion (all P < .005, Supplementary Fig. S5). The correlations between densities of different myeloid cell subtypes were low to moderate (Supplementary Fig. S6).

IDO and ARG1 Expression Patterns

We next examined IDO and ARG1 expression patterns. IDO was mainly expressed by monocytic cells (4.1% of all monocytic cells), and the expression was enriched in mature monocytic cells (4.8% of HLADR$^+$ monocytic cells and 0.64% of HLADR$^-$ monocytic cells). Accordingly, IDO$^+$ monocytic cell density was more highly correlated with HLADR$^+$ and FCGR3$^+$ (R = 0.52 and R = 0.34) monocytic cells than with HLADR$^-$ and FCGR3$^-$ (R = 0.13 and R = 0.04) monocytic cells, respectively (Supplementary Fig. S6). In addition to monocytic cells, a small number of tumor cells (2.7%) expressed IDO. There was a strong positive correlation between IDO$^+$ monocytic cell density and IDO$^+$ tumor cell percentage (R = 0.62) (Supplementary Fig. S6). ARG1 was primarily expressed by granulocytes, of which 81% were ARG1$^+$. Furthermore, ARG1 was more likely expressed by FCGR3$^+$ neutrophils than FCGR3$^-$ granulocytes (87% and 13%, respectively). Accordingly, the densities of ARG1$^+$ and FCGR3$^+$ neutrophils were closely correlated (R = 0.90) (Supplementary Fig. S6). The correlations of IDO$^+$ monocytic cell and ARG1$^+$ granulocyte densities with CD3$^+$ and CD8$^+$ T cell densities were further examined in 807 tumors that were successfully analyzed for these immune cell types in both the tumor center and the invasive margin. IDO$^+$ monocytic cell densities were moderately correlated with T cell densities in both tumor compartments, whereas ARG1$^+$ granulocyte densities showed lower correlation with T cell densities (Supplementary Fig. S7).

We analyzed the associations of clinicopathological characteristics with the density of IDO$^+$ monocytic cells (Table 1), IDO$^+$ tumor cell percentage (Supplementary Table S1), and the density of ARG1$^+$ granulocytes (Supplementary Table S2). Higher densities of IDO$^+$ monocytic cells and ARG1$^+$ granulocytes and higher IDO$^+$ tumor cell percentage were associated with low stage, absence of lymphovascular invasion, and MMR deficiency. Higher density of granulocytes and higher IDO$^+$ tumor cell percentage were associated with high tumor grade and *BRAF* mutation. Furthermore, higher density of IDO$^+$ monocytic cells was associated with operation in 2011-2015, and higher IDO$^+$ tumor cell

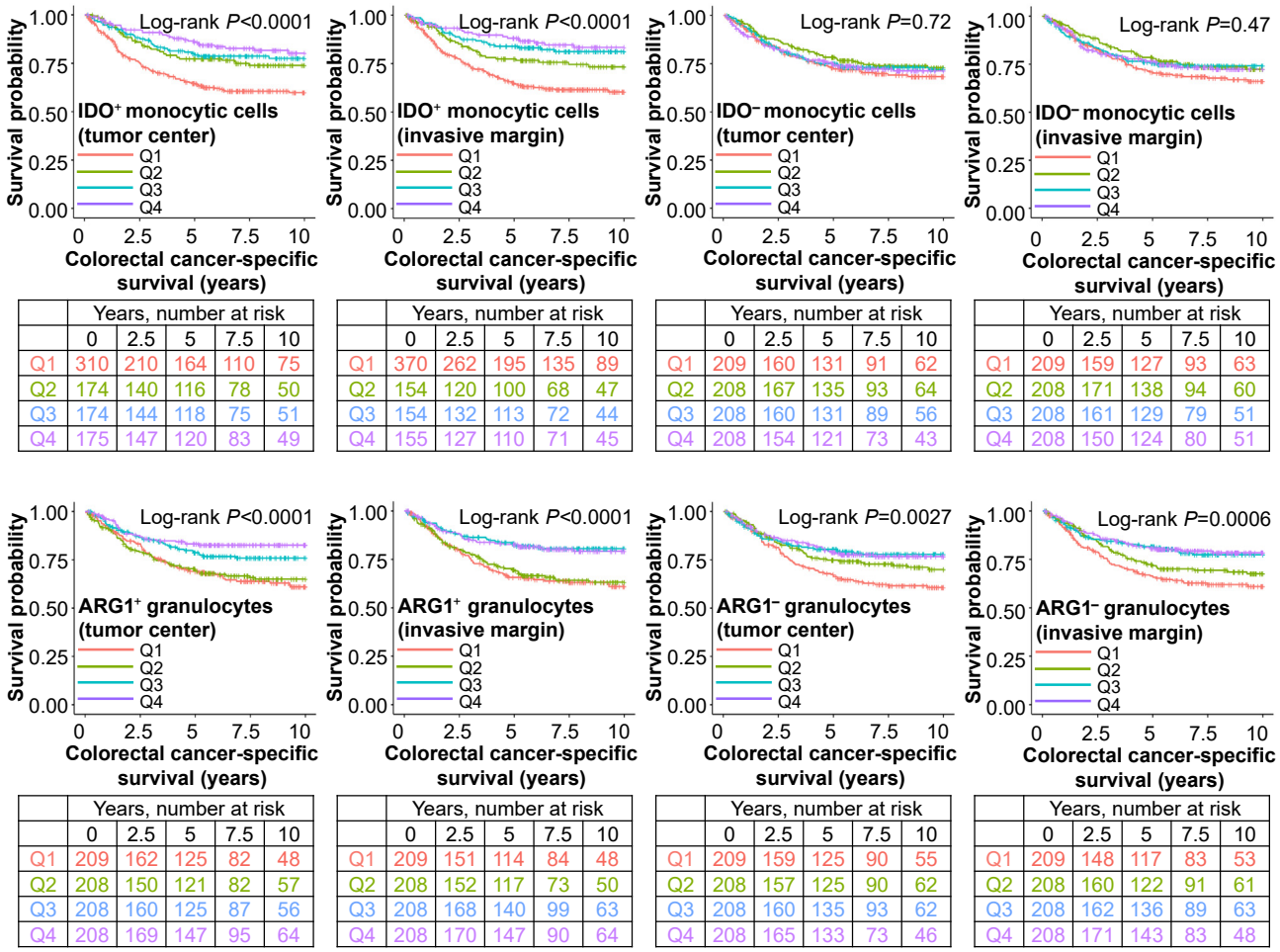

Figure 2.
Kaplan-Meier cancer-specific survival curves for the IDO$^+$ and IDO$^-$ monocytic cell and ARG1$^+$ and ARG1$^-$ granulocyte densities in the tumor center and in the invasive margin. The densities were divided into ordinal categories from low (Q1) to high (Q4). Statistical significance was determined with log-rank test.

percentage was associated with tumor location in the proximal colon. The associations between clinicopathologic features and IDO$^+$ and IDO$^-$ monocytic cells, as well as ARG1$^+$ and ARG1$^-$ granulocytes, in the tumor center and the invasive margin are shown in Supplementary Figure S8.

Survival Analyses

We examined the prognostic value of IDO and ARG1 expression, along with monocytic cell, granulocyte, and mast cell populations defined with various marker combinations. The total number of deaths was 477 (57%), including 224 (27%) cancer-specific deaths. The median follow-up time for censored cases was 10.1 years (IQR, 6.6-13.0). The overall density of monocytic cells did not associate with survival in univariable (Supplementary Fig. S9; Table S3) or multivariable (Supplementary Table S3) models. However, higher density of IDO$^+$ monocytic cells was associated with favorable cancer-specific and overall survival both in univariable (Fig. 2; Table 2) and multivariable analyses (Table 2) (cancer-specific survival, tumor center: $P_{trend} = .0002$; multivariable hazard ratio [HR] for Q4 [vs Q1], 0.51; 95% CI, 0.33-0.79; invasive margin: P_{trend}=0.0015; multivariable HR for Q4 [vs Q1], 0.51; 95% CI, 0.31-0.83). Full multivariable Cox regression models for IDO$^+$ and IDO$^-$ monocytic cells with all variables are shown in Supplementary Table S4. When tumor epithelial and stromal compartments were examined separately, the point estimate was stronger in the stroma (Supplementary Table S5).

To gain insights into the prognostic significance of more detailed monocytic cell populations, we assessed the prognostic impact of HLADR (Supplementary Table S6) and FCGR3 (Supplementary Table S7) expression in all monocytic cells and IDO$^+$ monocytic cells. The positive prognostic value of IDO$^+$ monocytic cells remained in the mature (HLADR$^+$) but not in the immature (HLADR$^-$) subset, whereas the survival associations were quite similar for FCGR3$^+$ and FCGR3$^-$ monocytic cell subpopulations.

In addition to monocytic cells, the prognostic significance of IDO expression in tumor cells was assessed. Higher IDO$^+$ tumor cell percentage was associated with longer survival in univariable models both in the tumor center and in the invasive margin, but these associations did not remain significant in multivariable models (Supplementary Fig. S10).

Higher density of granulocytes associated with favorable cancer-specific survival in univariable analyses in both the tumor center and the invasive margin (Supplementary Fig. S9; Table S3), but not in multivariable models (Supplementary Table S3). Comparable results were observed for ARG1$^+$ (Fig. 2; Supplementary

Table 2
Univariable and multivariable Cox regression models for cancer-specific and overall survival according to densities of IDO^+ and IDO^- monocytic cells in the tumor center and the invasive margin

	No. of cases	Colorectal cancer-specific survival			Overall survival		
		No. of events	Univariable HR (95% CI)	Multivariable HR (95% CI)	No. of events	Univariable HR (95% CI)	Multivariable HR (95% CI)
Tumor center							
IDO^+ monocytic cell density	833	216			406		
Q1	303	109	1 (referent)	1 (referent)	175	1 (referent)	1 (referent)
Q2	177	42	0.56 (0.40-0.81)	0.58 (0.40-0.84)	76	0.63 (0.48-0.82)	0.68 (0.51-0.89)
Q3	176	36	0.49 (0.34-0.71)	0.53 (0.36-0.78)	76	0.64 (0.49-0.83)	0.60 (0.45-0.79)
Q4	177	29	0.38 (0.25-0.58)	0.51 (0.33-0.79)	79	0.64 (0.49-0.84)	0.69 (0.52-0.91)
P_{trend}			<0.0001	0.0002		0.0003	0.0012
IDO^- monocytic cell density	833	216			406		
Q1	209	60	1 (referent)	1 (referent)	109	1 (referent)	1 (referent)
Q2	208	50	0.81 (0.55-1.18)	0.92 (0.63-1.35)	93	0.83 (0.63-1.10)	0.91 (0.69-1.21)
Q3	208	53	0.88 (0.61-1.28)	0.87 (0.59-1.26)	96	0.90 (0.68-1.18)	0.87 (0.65-1.15)
Q4	208	53	0.93 (0.74-1.34)	0.96 (0.65-1.42)	108	1.08 (0.83-1.41)	0.97 (0.73-1.28)
P_{trend}			0.78	0.73		0.50	0.73
Invasive margin							
IDO^+ monocytic cell density	833	216			406		
Q1	364	130	1 (referent)	1 (referent)	204	1 (referent)	1 (referent)
Q2	156	37	0.60 (0.42-0.87)	0.77 (0.53-1.12)	70	0.72 (0.55-0.94)	0.79 (0.60-1.04)
Q3	156	27	0.41 (0.27-0.63)	0.62 (0.40-0.96)	66	0.63 (0.48-0.84)	0.70 (0.53-0.94)
Q4	157	22	0.34 (0.22-0.54)	0.51 (0.31-0.83)	66	0.65 (0.49-0.86)	0.66 (0.49-0.90)
P_{trend}			<0.0001	0.0015		0.0002	0.0024
IDO^- monocytic cell density	833	216			406		
Q1	209	64	1 (referent)	1 (referent)	102	1 (referent)	1 (referent)
Q2	208	51	0.77 (0.53-1.11)	1.07 (0.73-1.56)	97	0.92 (0.70-1.22)	1.11 (0.84-1.49)
Q3	208	50	0.79 (0.55-1.15)	1.05 (0.72-1.55)	105	1.07 (0.82-1.41)	1.17 (0.88-0.56)
Q4	208	51	0.83 (0.57-1.20)	0.87 (0.59-1.28)	102	1.07 (0.81-1.41)	1.00 (0.75-1.33)
P_{trend}			0.35	0.51		0.42	0.93

The densities were divided into ordinal quartile categories from low (Q1) to high (Q4). Multivariable Cox proportional hazards regression models were adjusted for sex (male, female), age (<65, 65-75, and >75 years), year of operation (2000-2005, 2006-2010, and 2011-2015), tumor location (proximal colon, distal colon, and rectum), stages (I-II, III, and IV), tumor grade (well/moderately differentiated and poorly differentiated), lymphovascular invasion (negative or positive), MMR status (proficient or deficient), and *BRAF* status (wild type or mutant). P_{trend} values were calculated by using the 4 categories of immune cell densities as continuous variables in univariable and multivariable Cox proportional hazard regression models.

Table S8) and $FCGR3^+$ subpopulations (Supplementary Table S9). However, higher density of $ARG1^+FCGR3^+$ neutrophils in the tumor center was also significantly associated with longer cancer-specific survival in multivariable analysis (P_{trend} = .0020; HR, 0.49; 95% CI, 0.31-0.76; Supplementary Table S9). Higher mast cell density in the invasive margin was associated with longer cancer-specific survival in univariable analyses (Supplementary Fig. S9; Table S3), but not in multivariable models (Supplementary Table S3).

In secondary analyses, we examined the survival association of IDO^+ monocytic cells and $ARG1^+$ granulocytes in the strata of MMR status and stage. The survival association of IDO^+ monocytic cell density did not statistically significantly differ by MMR status ($P_{interaction}$ > .08) (Supplementary Table S10) or stage ($P_{interaction}$ > .17) (Supplementary Table S11). The survival association of $ARG1^+$ granulocyte density did not statistically significantly differ by MMR status ($P_{interaction}$ > .57) (Supplementary Table S12), but $ARG1^+$ granulocytes appeared to predict survival in stages I to III tumors and not in stage IV tumors ($P_{interaction}$ = .047 for multivariable cancer-specific survival models (Supplementary Table S13).

To assess the potential effect of the number of tissue microarray cores analyzed, we conducted survival analyses for the densities of IDO^+ monocytic cells and $ARG1^+$ granulocytic cells stratified by the number of analyzed cores (2-3 vs 4) (Supplementary Tables S14 and S15). The prognostic value did not statistically significantly differ by the number of analyzed tumor cores ($P_{interaction}$ > .24 for IDO^+ monocytic cells, $P_{interaction}$ > .32 for $ARG1^+$ granulocytes).

Spatial Analyses

We measured spatial arrangement of myeloid cells relative to tumor cells by using the NND analysis and found that granulocytes were significantly closer to tumor cells than monocytic cells and mast cells. Furthermore, $ARG1^-$ granulocytes were closer to tumor cells than $ARG1^+$ granulocytes, and IDO^+ monocytic cells were closer than IDO^- monocytic cells. However, the average NNDs from IDO^+ monocytic cells or $ARG1^+$ granulocytes to tumor cells did not associate with colorectal cancer-specific survival (Fig. 3).

Single-Cell RNA Transcriptomic Analysis for IDO1 Expression

To further characterize the factors potentially contributing to the association between higher IDO expression and better outcome, we analyzed *IDO1* expression in single-cell RNA transcriptomic data. Using previously determined cell communities (Fig. 4A),[19] we measured the expression of *IDO1* mRNA across the immune cells, tumor cells, and stromal cells. As IDO is a key regulator of tryptophan catabolism, we measured the activity of

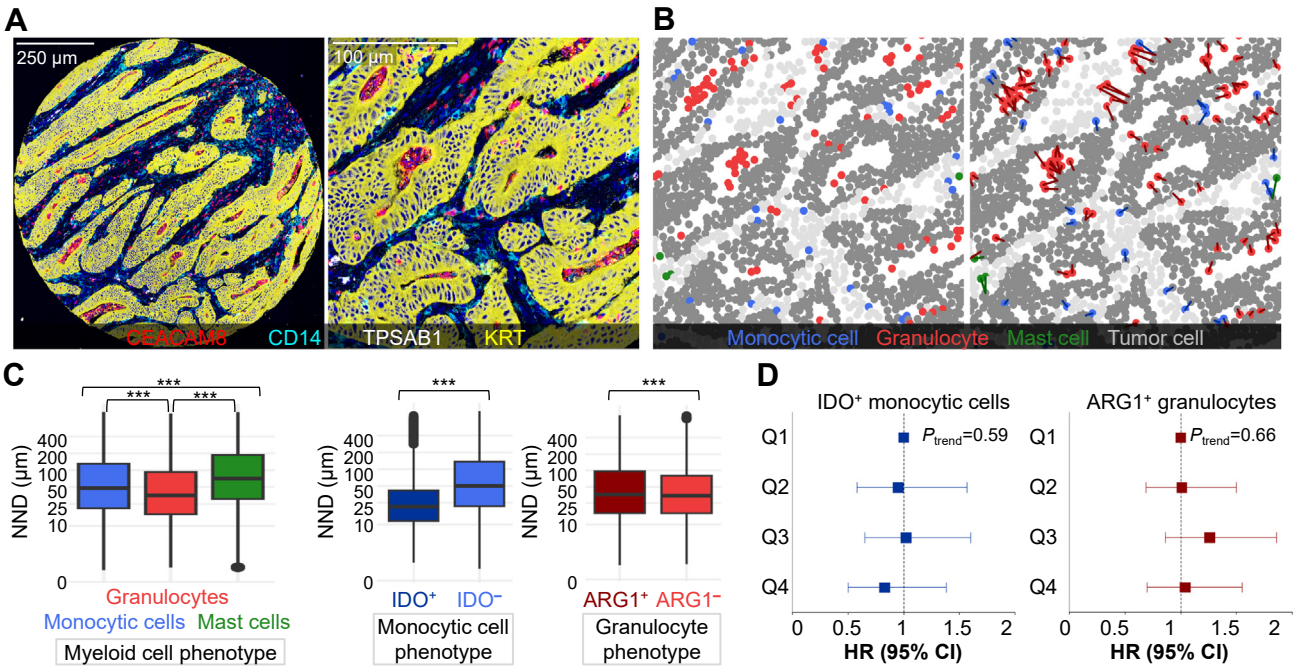

Figure 3.
Nearest neighbor distance (NND) analysis for myeloid cells and tumor cells. (A) Example multiplex-immunohistochemistry image representing granulocytes (CEACAM8$^+$), monocytic cells (CD14$^+$), mast cells (TPSAB1$^+$), and tumor cells (KRT$^+$) in one tumor core and in close-up view. (B) Cell phenotyping maps and NNDs calculated from each myeloid cell to the closest tumor cell. (C) Boxplots representing the average distribution of NNDs across all tumor images ($N = 2813$). The statistical significance was tested with Wilcoxon rank-sum test. *** $P < .0001$. (D) Forest plots visualizing colorectal cancer-specific survival according to average NNDs for 2 specific immune cell types in each tumor. NNDs were divided into ordinal quartiles from short (Q1) to long (Q4) NND. We only included tumors with at least one specific immune cell ($N = 626$ for IDO$^+$ monocytic cells and $N = 821$ for ARG1$^+$ granulocytes). Multivariable Cox proportional hazards regression models were represented with hazard ratios (HRs) and 95% CI as whiskers. The models were adjusted for sex (male and female), age (<65, 65–75, and >75 years), year of operation (2000-2005, 2006-2010, and 2011-2015), tumor location (proximal colon, distal colon, and rectum), stages (I-II, III, and IV), tumor grade (well/moderately differentiated and poorly differentiated), lymphovascular invasion (negative or positive), MMR status (proficient or deficient), and *BRAF* status (wild type or mutant).

the tryptophan metabolism pathway (GO:0006568). The activities of *IDO1* (Fig. 4B) and tryptophan metabolism (Fig. 4C) were highest in monocytes and dendritic cells. Next, we calculated the median percentage of *IDO1*$^+$ cells within each cell community. *IDO1*$^+$ fraction was the highest on dendritic cells, as almost 30% of all patients' dendritic cells, by median, were *IDO1*$^+$ (Fig. 4D). To find the enriched cell processes, we conducted a gene set enrichment analysis for *IDO1*$^+$ (vs *IDO1*$^-$) monocytes. We found that several IFNG-regulated immunostimulatory pathways were positively enriched in *IDO1*$^+$ monocytes (Fig. 4E). Thus, we further studied the association between *IDO1* and *IFNG* by dividing tumors based on high and low monocytic cell *IDO1* expression. *IFNG* was strongly expressed in T cells within tumors exhibiting high *IDO1* activity in monocytes. In tumors with low monocytic *IDO1* activity, lymphocyte *IFNG* expression was lower, and the population of T cells was diminished (Fig. 4F). To investigate the impact of high *IDO1* expression on cellular interactions, we compared the number of interactions between tumors with higher and lower *IDO1* expressions. High *IDO1* expression was associated with stronger interactions between most immune cells, although interactions between granulocytes and other cell types were diminished (Fig. 4G).

Discussion

In the present study, we used a detailed immunohistochemical multimarker technique and machine learning–based image analysis to comprehensively characterize IDO and ARG1 expression patterns and myeloid immune cell infiltration in the colorectal cancer microenvironment of 833 tumors. We also used publicly available single-cell mRNA data for 62 colorectal cancer patients to further assess functional pathways associated with *IDO1* expression. These analyses improve our understanding of the spatial distribution and implications of IDO and ARG1 within the colorectal cancer microenvironment and offer potential insights into tumor immunology, treatment development, and biomarker discovery.

We found that IDO was mainly expressed by monocytic cells and tumor cells, whereas ARG1 was expressed by granulocytes. Although the overall density of monocytic cells was not prognostic, higher infiltration of IDO$^+$ monocytic cells both in the tumor center and the invasive margin was associated with improved cancer-specific survival, independent of potential confounding factors such as MMR status and stage. Higher percentage of IDO$^+$ tumor cells was also associated with longer survival but only in univariable models. Our findings were in line with previous studies in colorectal[21,22] and other solid cancers[23-25] reporting the association between high IDO expression and prolonged survival. In contrast, some studies have reported an association between increased IDO expression and poor survival in colorectal cancer[8,26] and some other solid cancers.[7] The diversity of the analysis methods may account for this discrepancy, and to our knowledge, no previous studies have specifically evaluated CD14$^+$IDO$^+$ monocytic cells, which is impossible using conventional single-color immunohistochemistry.

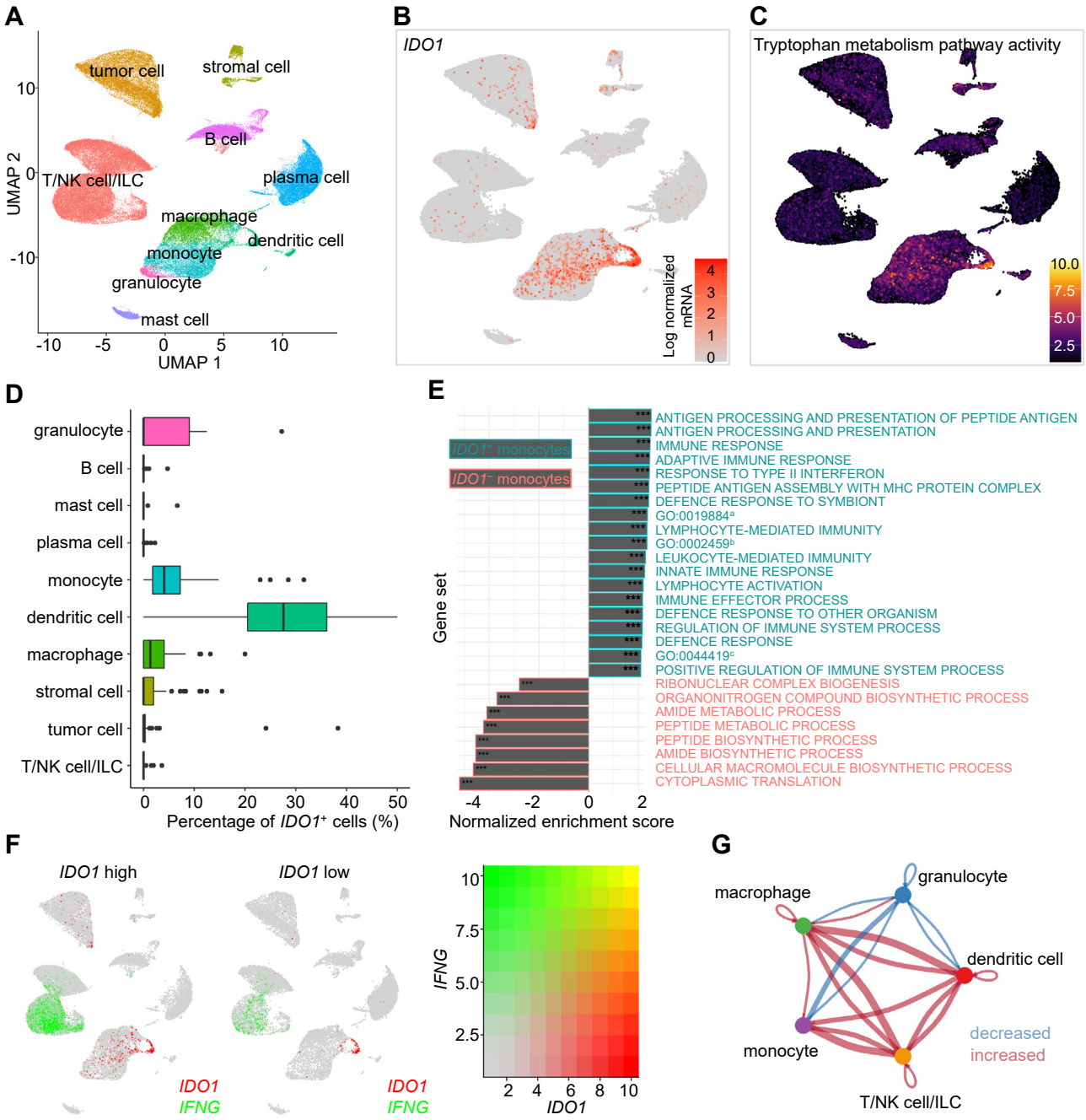

Figure 4.
The distribution of *IDO1* expression in immune cell subtypes and tumor cells. (A) Uniform manifold approximation and projection (UMAP) representation for cell communities clustering in 62 tumors. (B) The expression level of *IDO1* in cell communities. (C) The activity of tryptophan metabolism pathway in cell communities. (D) Boxplots representing the percentage of *IDO1* active cells in cell populations ($N = 62$ tumors). (E) Bar plot of the pathway enrichment analysis shows pathways activated in *IDO1*$^+$ monocytes in green and those activated in *IDO1*$^-$ monocytes in red. ***$P < .0001$. [a]ANTIGEN PROCESSING AND PRESENTATION OF EXOGENOUS ANTIGEN. [b]ADAPTIVE IMMUNE RESPONSE BASED ON SOMATIC RECOMBINATION OF IMMUNE RECEPTORS BUILT FROM LEUCINE-RICH REPEAT DOMAINS. [c]BIOLOGICAL PROCESS INVOLVED IN INTERSPECIES INTERACTION BETWEEN ORGANISMS. (F) *IFNG* activity in tumors with high and low *IDO1* activity. (G) The number of cellular interactions between immune cells in *IDO1* high tumors. The width of the edges represents the number of communications. Red color indicates increased number of communications and blue decreased number of communications in *IDO1* high tumors compared to *IDO1* low tumors. ILC, innate lymphoid cell; NK, natural killer; UMAP, Uniform manifold approximation and projection.

Higher granulocyte density in the tumor center and the invasive margin was a favorable prognostic factor in univariable analyses, supported by several previous studies in colorectal cancer.[17,27-31] However, conflicting findings of the association between higher granulocyte density and worse colorectal cancer survival have also been reported.[32] Our study benefited from the multimarker approach, which enabled us to define granulocyte subpopulations based on simultaneous expression of CEACAM8, FCGR3, and ARG1. The majority of granulocytes were FCGR3$^+$ neutrophils and also expressed ARG1. Higher density of CEACAM8$^+$FCGR3$^+$ARG1$^+$ neutrophils in the tumor center was significantly associated with prolonged cancer-specific survival also in multivariable analysis. As we further assessed the prognostic value of ARG1$^+$ granulocytes in strata of the stage, the

independent survival association remained only in the lower stages (I-III) tumors. These findings suggest that neutrophils, many of which express ARG1$^+$, may lose their beneficial antitumor effect during the progression of colorectal cancer.

The association between higher IDO and ARG1 expression and longer cancer-specific survival is paradoxical, as IDO and ARG1 are thought to be immunosuppressive enzymes.[33] The factors accounting for this association are not obvious, but our findings and previous literature provide some potential explanations. It has been hypothesized that increased expression of IDO and ARG1 could be a compensatory, intrinsic negative feedback reaction to the generally strengthened antitumor immune response in the tumor microenvironment.[22,34-36] In accordance with this hypothesis, we found that immunostimulatory pathways were enriched in *IDO1*$^+$ monocytes. IFNG is a molecule contributing to several proinflammatory processes and has been suggested to induce IDO expression.[8,36,37] Our single-cell RNA analysis also supported an association between *IDO1* and *IFNG* expression, as cases with higher monocyte-derived *IDO1* expression were associated with higher numbers of T cells and with higher expression of *IFNG* on T cells compared with those with lower *IDO1* expression. A positive correlation between IDO$^+$ monocytic cells and T cells was also observed in the main cohort and has been reported in several previous studies.[22,36,38] Furthermore, it is known that certain cancer risk factors may paradoxically be linked with favorable survival among cancer patients, which is explained by the interpersonal heterogeneity of cancer.[39] In this study, we found that higher density of IDO$^+$ monocytic cells, higher percentage of IDO$^+$ tumor cells, and higher density of ARG1$^+$ granulocytes were associated with low stage and absence of lymphovascular invasion, which are known to be strong favorable prognostic indicators in colorectal cancer.[40] Therefore, higher expression of these immunosuppressive molecules could be a marker of a less aggressive tumor phenotype. Indeed, some cell types, such as ARG1$^+$ granulocytes, had a considerably weaker prognostic association after adjustment for other clinicopathologic features. However, IDO$^+$ monocytic cells remained significant in multivariable Cox regression models for cancer-specific survival after adjusting for a group of known prognostic indicators such as disease stage, tumor grade, lymphovascular invasion, MMR status, and *BRAF* status, supporting their independent prognostic value.

To our knowledge, this is the first study examining the myeloid cell infiltration along with IDO and ARG1 immunoregulatory enzymes in colorectal cancer using multiplex immunohistochemistry. However, some important limitations need to be considered. First, there are no standardized and fully specific markers for phenotyping myeloid cells, which complicates the interpretation of findings between different studies. However, we selected well-validated antibodies that were in clinical use at our pathology laboratory or utilized in previous studies. Second, we used tissue microarrays instead of whole tissue slides, which may not fully represent the whole tumor immune milieu.[41] However, we analyzed tumor cores taken from both the tumor center and the invasive margin and reached moderate-to-high core-to-core correlations. This suggested tissue microarray–based methods to be suitable for evaluating these immune cell infiltrates. Third, we used a cyclic staining assay, where the loss of tumor cores was higher than in standard immunohistochemical staining. Still, the size of our study cohort remained large, and the tissue microarray-based multiplex-immunohistochemistry analysis enabled us to analyze all samples cost-efficiently in one batch. Fourth, most patients are non-Hispanic white. Thus, our findings need to be confirmed in patients with non-White Caucasian ethnicities. Independent validation study is also required to confirm whether IDO1$^+$ monocytic cell densities could be used as a clinically relevant prognostic marker in colorectal cancer. Fifth, data on recurrence-free survival were not available for this study. Nevertheless, a long follow-up period enabled the assessment of long-term survival impact, based on cancer-specific and overall survival outcomes. Sixth, the patients underwent surgery over a 16-year period, during which cancer treatments have evolved, potentially influencing disease outcome and clinicopathologic features of the patients included in the cohort. To minimize potential bias, we included the year of operation as a covariate in the multivariable survival models.

This study has notable strengths. It included a large cohort of 833 colorectal cancers, with a comprehensive database from multiple previous studies,[12,13,34,42-45] and an independent single-cell RNA transcriptomic dataset with 62 colorectal cancers. We only included patients without neoadjuvant treatment to eliminate the possible bias related to its effects on the immune microenvironment, which however led to the underrepresentation of rectal cancers. Multiplex-immunohistochemistry analysis combined with machine learning-based image analysis enabled detailed phenotyping of cells using several markers and the study of spatial relationships between cell types, which cannot be done using conventional immunohistochemistry.[11]

In conclusion, our study provided detailed information about IDO and ARG1 expression patterns and myeloid cell infiltration in the colorectal cancer microenvironment. We found that the density of IDO-expressing monocytic cells was an independent favorable prognostic factor, and at the single-cell level, *IDO1* expression was strongly associated with *IFNG*-regulated immunostimulatory pathways. Our results provide insight into the complexity of colorectal cancer immunity and suggest that comprehensive characterization is necessary to dissect its effects on patient outcomes.

Author Contributions

H.E., S.A.V., S.O., J.A.N., J.B., T.K., and J.P.V. designed study concept; J.B., J.P.M., T.K., and J.P.V. provided resources; H.E., J.H., M.A., O.H., E.V.W., T.T.S., J.B., J.P.M., and J.P.V. were responsible for data curation; T.K. and J.P.V. supervised this study; H.E. and J.P.V. conducted formal analysis and acquired the funding; H.E., J.H., S.A.V., M.A., O.H., E.V.W., T.T.S., J.B., J.P.M., T.K., and J.P.V. conducted investigation; H.E., J.H., S.A.V., M.C.L., and J.P.V. visualized the data; H.E., J.H., S.A.V., .S.O., J.A.N., M.C.L., and J.P.V. contributed to the methodology; H.E., J.H., and J.P.V. wrote the original draft. All authors edited and approved the manuscript.

Data Availability

Single-cell RNA-seq counts and metadata were publicly available at GEO (GSE178341) and at Broad Institute Single Cell Portal (https://singlecell.broadinstitute.org/single_cell, dataset c295). Other data generated and/or analyzed during this study are not publicly available. The sharing of data will require approval from relevant ethics committees and/or biobanks. Further information including the procedures to obtain and access data of Finnish Biobanks are described at https://finbb.fi/en/fingenious-service.

Funding

This study was funded by Cancer Foundation Finland (59-5619 to J.P.V. and to H.E.), Emil Aaltonen Foundation (220022K to H.E.), Orion Research Foundation sr (to H.E.), Päivikki and Sakari

Sohlberg Foundation (to H.E.), Sigrid Jusélius Foundation (230229 to J.P.V.), and the State Research Funding (to J.P.V. and to H.E.). T.T.S. was supported by research grants from Jane and Aatos Erkko Foundation, Sigrid Jusélius Foundation, Finnish Medical Foundation, Emil Aaltonen Foundation, Cancer Foundation Finland, Relander Foundation, and the State Research Funding. The funders had no role in study design, data collection and analysis, decision to publish, or preparation of the manuscript.

Declaration of Competing Interest

J.A. Nowak reports grant funding from Natera and consulting fees from Leica Biosystems. T.T. Seppälä reports a consultation fee from Amgen Finland and being a co-owner and CEO of Healthfund Finland Ltd, and the Clinical Advisory Board of LS Cancer Diag Ltd. The other authors declare no potential conflicts of interest.

Ethics Approval and Consent to Participate

The study was conducted according to the guidelines of the Declaration of Helsinki and approved by the hospital administration and the ethics board (Dnro13U/2011, 1/2016, 8/2020, and 2/2023), the Finnish Medicines Agency (Fimea), and the Central Finland Biobank (BB23-0172). The need to obtain informed consent from the study patients was waived (Dnro FIMEA/2023/001573, 4/2023).

Supplementary Material

The online version contains supplementary material available at https://doi.org/10.1016/j.modpat.2024.100450

References

1. Zhang J, Zou S, Fang L. Metabolic reprogramming in colorectal cancer: regulatory networks and therapy. *Cell Biosci*. 2023;13(1):25. https://doi.org/10.1186/s13578-023-00977-w
2. Ma Z, Lian J, Yang M, et al. Overexpression of Arginase-1 is an indicator of poor prognosis in patients with colorectal cancer. *Pathol Res Pract*. 2019;215(6):152383. https://doi.org/10.1016/j.prp.2019.03.012
3. Meireson A, Devos M, Brochez L. IDO Expression in cancer: different compartment, different functionality? *Front Immunol*. 2020;11:531491. https://doi.org/10.3389/fimmu.2020.531491
4. Bronte V, Zanovello P. Regulation of immune responses by L-arginine metabolism. *Nat Rev Immunol*. 2005;5(8):641–654. https://doi.org/10.1038/nri1668
5. Wei Z, Liu X, Cheng C, Yu W, Yi P. Metabolism of amino acids in cancer. *Front cell Dev Biol*. 2020;8:603837. https://doi.org/10.3389/fcell.2020.603837
6. Grzywa TM, Sosnowska A, Matryba P, et al. Myeloid cell-derived arginase in cancer immune response. *Front Immunol*. 2020;11(8):938. https://doi.org/10.3389/fimmu.2020.00938
7. Wang S, Wu J, Shen H, Wang J. The prognostic value of IDO expression in solid tumors: a systematic review and meta-analysis. *BMC Cancer*. 2020;20(1):471. https://doi.org/10.1186/s12885-020-06956-5
8. Brandacher G, Perathoner A, Ladurner R, et al. Prognostic value of indoleamine 2,3-dioxygenase expression in colorectal cancer: effect on tumor-infiltrating T cells. *Clin Cancer Res*. 2006;12(4):1144–1151. https://doi.org/10.1158/1078-0432.CCR-05-1966
9. Ma WJ, Wang X, Yan WT, et al. Indoleamine-2,3-dioxygenase 1/cyclooxygenase 2 expression prediction for adverse prognosis in colorectal cancer. *World J Gastroenterol*. 2018;24(20):2181–2190. https://doi.org/10.3748/wjg.v24.i20.2181
10. Munder M, Mollinedo F, Calafat J, et al. Arginase I is constitutively expressed in human granulocytes and participates in fungicidal activity. *Blood*. 2005;105(6):2549–2556. https://doi.org/10.1182/blood-2004-07-2521
11. Elliott LA, Doherty GA, Sheahan K, Ryan EJ. Human tumor-infiltrating myeloid cells: phenotypic and functional diversity. *Front Immunol*. 2017;8:86. https://doi.org/10.3389/fimmu.2017.00086
12. Elomaa H, Ahtiainen M, Väyrynen SA, et al. Spatially resolved multimarker evaluation of CD274 (PD-L1)/PDCD1 (PD-1) immune checkpoint expression and macrophage polarisation in colorectal cancer. *Br J Cancer*. 2023;128(11):2104–2115. https://doi.org/10.1038/s41416-023-02238-6
13. Elomaa H, Ahtiainen M, Väyrynen SA, et al. Prognostic significance of spatial and density analysis of T lymphocytes in colorectal cancer. *Br J Cancer*. 2022;127(3):514–523. https://doi.org/10.1038/s41416-022-01822-6
14. Fujiyoshi K, Bruford EA, Mroz P, et al. Opinion: standardizing gene product nomenclature-a call to action. *Proc Natl Acad Sci USA*. 2021;118(3):1–5. https://doi.org/10.1073/pnas.2025207118
15. Bankhead P, Loughrey MB, Fernández JA, et al. QuPath: open source software for digital pathology image analysis. *Sci Rep*. 2017;7(1):16878. https://doi.org/10.1038/s41598-017-17204-5
16. Schindelin J, Arganda-Carreras I, Frise E, et al. Fiji: an open-source platform for biological-image analysis. *Nat Methods*. 2012;9(7):676–682. https://doi.org/10.1038/nmeth.2019
17. Väyrynen JP, Lau MC, Haruki K, et al. Prognostic significance of immune cell populations identified by machine learning in colorectal cancer using routine hematoxylin and eosin-stained sections. *Clin Cancer Res*. 2020;26(16):4326–4338. https://doi.org/10.1158/1078-0432.CCR-20-0071
18. Benjamin DJ, Berger JO, Johannesson M, et al. Redefine statistical significance. *Nat Hum Behav*. 2018;2(1):6–10. https://doi.org/10.1038/s41562-017-0189-z
19. Pelka K, Hofree M, Chen JH, et al. Spatially organized multicellular immune hubs in human colorectal cancer. *Cell*. 2021;184(18):4734–4752.e20. https://doi.org/10.1016/j.cell.2021.08.003
20. Jin S, Guerrero-Juarez CF, Zhang L, et al. Inference and analysis of cell-cell communication using CellChat. *Nat Commun*. 2021;12(1):1088. https://doi.org/10.1038/s41467-021-21246-9
21. Lee SJ, Jun SY, Lee IH, et al. CD274, LAG3, and IDO1 expressions in tumor-infiltrating immune cells as prognostic biomarker for patients with MSI-high colon cancer. *J Cancer Res Clin Oncol*. 2018;144(6):1005–1014. https://doi.org/10.1007/s00432-018-2620-x
22. Schollbach J, Kircher S, Wiegering A, et al. Prognostic value of tumour-infiltrating CD8+ lymphocytes in rectal cancer after neoadjuvant chemoradiation: is indoleamine-2,3-dioxygenase (IDO1) a friend or foe? *Cancer Immunol Immunother*. 2019;68(4):563–575. https://doi.org/10.1007/s00262-019-02306-y
23. Ma W, Duan H, Zhang R, et al. High expression of indoleamine 2, 3-dioxygenase in adenosquamous lung carcinoma correlates with favorable patient outcome. *J Cancer*. 2019;10(1):267–276. https://doi.org/10.7150/jca.27507
24. Ishio T, Goto S, Tahara K, Tone S, Kawano K, Kitano S. Immunoactivative role of indoleamine 2,3-dioxygenase in human hepatocellular carcinoma. *J Gastroenterol Hepatol*. 2004;19(3):319–326. https://doi.org/10.1111/j.1440-1746.2003.03259.x
25. Jacquemier J, Bertucci F, Finetti P, et al. High expression of indoleamine 2,3-dioxygenase in the tumour is associated with medullary features and favourable outcome in basal-like breast carcinoma. *Int J cancer*. 2012;130(1):96–104. https://doi.org/10.1002/ijc.25979
26. Ferdinande L, Decaestecker C, Verset L, et al. Clinicopathological significance of indoleamine 2,3-dioxygenase 1 expression in colorectal cancer. *Br J Cancer*. 2012;106(1):141–147. https://doi.org/10.1038/bjc.2011.513
27. Väyrynen JP, Haruki K, Väyrynen SA, et al. Prognostic significance of myeloid immune cells and their spatial distribution in the colorectal cancer microenvironment. *J Immunother cancer*. 2021;9(4):e002297. https://doi.org/10.1136/jitc-2020-002297
28. Governa V, Trella E, Mele V, et al. The interplay between neutrophils and CD8+ T cells improves survival in human colorectal cancer. *Clin Cancer Res*. 2017;23(14):3847–3858. https://doi.org/10.1158/1078-0432.CCR-16-2047
29. Galdiero MR, Bianchi P, Grizzi F, et al. Occurrence and significance of tumor-associated neutrophils in patients with colorectal cancer. *Int J cancer*. 2016;139(2):446–456. https://doi.org/10.1002/ijc.30076
30. Berry RS, Xiong MJ, Greenbaum A, et al. High levels of tumor-associated neutrophils are associated with improved overall survival in patients with stage II colorectal cancer. *PLoS One*. 2017;12(12):e0188799. https://doi.org/10.1371/journal.pone.0188799
31. Droeser RA, Hirt C, Eppenberger-Castori S, et al. High myeloperoxidase positive cell infiltration in colorectal cancer is an independent favorable prognostic factor. *PLoS One*. 2013;8(5):e64814. https://doi.org/10.1371/journal.pone.0064814
32. Wikberg ML, Ling A, Li X, Å Öberg, Edin S, Palmqvist R. Neutrophil infiltration is a favorable prognostic factor in early stages of colon cancer. *Hum Pathol*. 2017;68(2017):193–202. https://doi.org/10.1016/j.humpath.2017.08.028
33. Mondanelli G, Iacono A, Allegrucci M, Puccetti P, Grohmann U. Immunoregulatory interplay between arginine and tryptophan metabolism in health and disease. *Front Immunol*. 2019;10:1565. https://doi.org/10.3389/fimmu.2019.01565
34. Ahtiainen M, Wirta EV, Kuopio T, et al. Combined prognostic value of CD274 (PD-L1)/PDCDI (PD-1) expression and immune cell infiltration in colorectal cancer as per mismatch repair status. *Mod Pathol*. 2019;32(6):866–883. https://doi.org/10.1038/s41379-019-0219-7

35. Lazarus J, Oneka MD, Barua S, et al. Mathematical modeling of the metastatic colorectal cancer microenvironment defines the importance of cytotoxic lymphocyte infiltration and presence of PD-L1 on antigen presenting cells. *Ann Surg Oncol*. 2019;26(9):2821−2830. https://doi.org/10.1245/s10434-019-07508-3
36. Spranger S, Spaapen RM, Zha Y, et al. Up-regulation of PD-L1, IDO, and T(regs) in the melanoma tumor microenvironment is driven by CD8(+) T cells. *Sci Transl Med*. 2013;5(200):200ra116. https://doi.org/10.1126/scitranslmed.3006504
37. Schalper KA, Carvajal-Hausdorf D, McLaughlin J, et al. Differential expression and significance of PD-L1, IDO-1, and B7-H4 in human lung cancer. *Clin Cancer Res*. 2017;23(2):370−378. https://doi.org/10.1158/1078-0432.CCR-16-0150
38. Zhang ML, Kem M, Mooradian MJ, et al. Differential expression of PD-L1 and IDO1 in association with the immune microenvironment in resected lung adenocarcinomas. *Mod Pathol*. 2019;32(4):511−523. https://doi.org/10.1038/s41379-018-0160-1
39. Nishihara R, VanderWeele TJ, Shibuya K, et al. Molecular pathological epidemiology gives clues to paradoxical findings. *Eur J Epidemiol*. 2015;30(10):1129−1135. https://doi.org/10.1007/s10654-015-0088-4
40. Zlobec I, Lugli A. Prognostic and predictive factors in colorectal cancer. *Postgrad Med J*. 2008;84(994):403−411. https://doi.org/10.1136/jcp.2007.054858
41. Giltnane JM, Rimm DL. Technology insight: identification of biomarkers with tissue microarray technology. *Nat Clin Pract Oncol*. 2004;1(2):104−111. https://doi.org/10.1038/ncponc0046
42. Seppälä TT, Böhm JP, Friman M, et al. Combination of microsatellite instability and BRAF mutation status for subtyping colorectal cancer. *Br J Cancer*. 2015;112(12):1966−1975. https://doi.org/10.1038/bjc.2015.160
43. Porkka N, Lahtinen L, Ahtiainen M, et al. Epidemiological, clinical and molecular characterization of Lynch-like syndrome: a population-based study. *Int J cancer*. 2019;145(1):87−98. https://doi.org/10.1002/ijc.32085
44. Wirta EV, Seppälä T, Friman M, et al. Immunoscore in mismatch repair-proficient and -deficient colon cancer. *J Pathol Clin Res*. 2017;3(3):203−213. https://doi.org/10.1002/cjp2.71
45. Kellokumpu I, Kairaluoma M, Mecklin JP, et al. Impact of age and comorbidity on multimodal management and survival from colorectal cancer: a population-based study. *J Clin Med*. 2021;10(8):1751. https://doi.org/10.3390/jcm10081751